

# Matter-wave gap vortices in optical lattices

Elena A. Ostrovskaya and Yuri S. Kivshar

*Nonlinear Physics Group and ARC Centre of Excellence for Quantum-Atom Optics,  
Research School of Physical Sciences and Engineering,  
Australian National University, Canberra ACT 0200, Australia*

We predict the existence of spatially localized nontrivial topological states of a Bose-Einstein condensate with repulsive atomic interactions confined by an optical lattice. These nonlinear localized states, *matter-wave gap vortices*, possess a vortex-like phase dislocation and exist in the *gaps* of the matter-wave bandgap spectrum due to the Bragg scattering. We discuss the structure, stability, and formation dynamics of the gap vortices in the case of two-dimensional optical lattices.

Similarities between the physics of coherent light and matter waves can be successfully used to understand and predict nonlinear dynamics of weakly interacting Bose-Einstein condensates (BECs) in optical lattices [1, 2, 3, 4, 5]. In analogy with periodic photonic structures for light waves, such as photonic crystals, optical lattices form band-gap structures which modify diffraction and localization properties of BECs with both attractive and repulsive atomic interactions. In the case of a repulsive BEC, optical lattices offer *two intriguing possibilities*. First, they enable nonlinear localization of a repulsive condensate in the gaps of the Bloch-wave spectrum, without a confining harmonic potential [6, 7]. Secondly, by manipulating the band gaps of the lattice Bloch-wave spectrum, the degree of BEC localization can be varied from a low density state spread out across the lattice to a condensate droplet tightly bound in a vicinity of a single lattice well. Both the BEC diffraction management in shallow one-dimensional (1D) optical lattices [3, 4] and the nonlinear localization of a BEC with repulsive atomic interactions [8] were observed in experiments.

One of the fundamental questions is how distinctively superfluid properties of weakly interacting condensates, e.g., the dynamics of vortices [9], are modified by an optical lattice, and whether it is possible to spatially localize a BEC wavepacket with a nontrivial topological phase in a lattice. Several parallel studies in the physics of coherent optical [10] and matter waves [11] suggest that localization of topological defects is possible for an *attractive* condensate within a *tightly binding* lattice. The localized vortices in the attractive condensate would be analogous to bright optical vortex solitons predicted to exist in total internal reflection gaps of dynamical photonic lattices [10, 12] and photonic crystal fibers [13] with *focusing* nonlinearity, and recently observed in experiments on photonic lattices [14]. Localization of vortices in the *repulsive* BEC confined by a *shallow* lattice, i.e. when the standard mechanisms of spatial confinement are *absent*, remains an open problem.

In this Letter we show that nonlinear localization of a repulsive BEC with a phase defect is possible within a complete Bragg-reflection gap of the Bloch-wave spectrum. The resulting *matter-wave gap vortices* are spa-

tially localized and dynamically stable. Due to their finite spatial extent, which is much smaller than the dimensions of the loose confining trap, the localized gap vortices can also be termed “bright” vortices, by analogy with vortex rings of light in nonlinear optical media. Surprisingly, the density and phase structure of a localized lattice vortex is determined by the features of delocalized “dark” vortices, which reside on a spatially extended periodic background of matter-wave Bloch states.

The framework of our analysis is set by the mean-field Gross-Pitaevskii model of an anisotropic BEC cloud loaded into a two-dimensional optical lattice potential,

$$i\frac{\partial\Psi}{\partial t} = \{-\nabla_{\perp}^2 + V(x, y) + |\Psi|^2\}\Psi. \quad (1)$$

This equation is obtained by assuming a tight confinement in the direction perpendicular to the lattice (“pancake” trapping geometry) and a standard dimensionality reduction procedure (see, e.g., Ref. [2]). It is made dimensionless by using the characteristic length  $a_L = d/\pi$ , energy  $E_L = \hbar^2/2ma_L^2$ , and time  $\omega_L^{-1} = \hbar/E_L$  scales of the lattice, where  $d$  is the lattice period, and  $m$  the mass of the trapped atoms. The wavefunction is scaled as  $\Psi \rightarrow \Psi\sqrt{g_{2D}}$ , where the rescaled 2D interaction strength is  $g_{2D} = 4\sqrt{2}\pi a_s/a_L$ , and  $a_s$  is the s-wave scattering length. To eliminate any possible localization effects which are *not* due to the optical lattice, we *removed* from consideration any additional trapping of the condensate in the directions of the lattice. The trapping potential is therefore taken in the form,  $V(x, y) = V_0[\sin^2(x + \theta) + \sin^2(y + \theta)]$ .

Stationary states of a BEC are described by solutions of Eq. (1) of the form:  $\Psi(\mathbf{r}, t) = \psi(\mathbf{r})\exp(-i\mu t)$ , where  $\mu$  is the chemical potential. Stationary states of the non-interacting BEC are found as  $\psi(\mathbf{r}) = \phi_{\mathbf{k}}(\mathbf{r})\exp(i\mathbf{k}\mathbf{r})$ , where the wavevector  $\mathbf{k}$  belongs to the Brillouine zone (BZ) of the square lattice, and  $\phi_{\mathbf{k}}(\mathbf{r}) = \phi_{\mathbf{k}}(\mathbf{r} + \mathbf{d})$  is a periodic (Bloch) function with the periodicity of the lattice. The band-gap structure of spectrum,  $\mu(\mathbf{k})$ , of the atomic Bloch waves in the optical lattice is shown in the top panel of Fig. 1, in the reduced zone representation usually employed in the theory of crystalline solids.

In a homogeneous BEC, a vortex with the topological charge one is characterized by a  $2\pi$  phase winding around

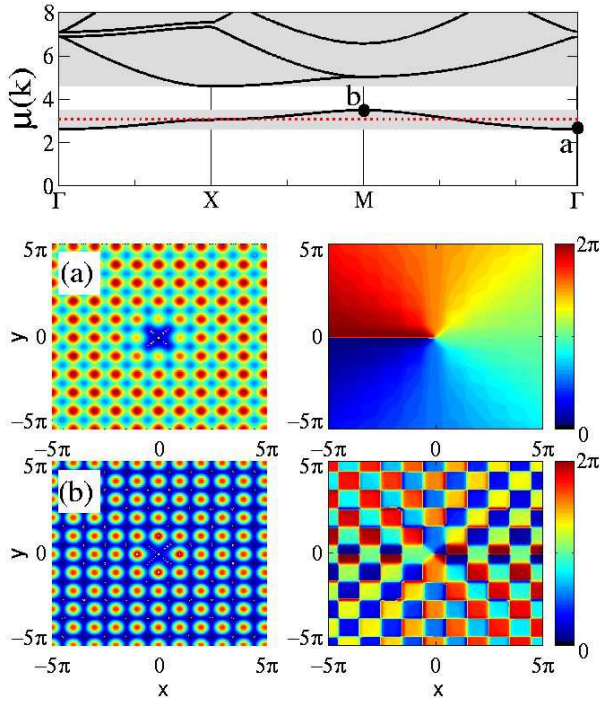


FIG. 1: Top: Matter-wave Bloch spectrum in a 2D optical lattice ( $V_0 = 3.0$ ) shown along the edges of the irreducible BZ,  $\Gamma(k_x = 0, k_y = 0) \rightarrow X(k_x = 1, k_y = 0) \rightarrow M(k_x = 1, k_y = 1)$ . Shaded and open areas show bands and gaps, respectively. Bottom: examples of the condensate wavefunctions,  $|\psi|^2$ , (red color codes maximum density) at the marked points of the dispersion curves, corresponding to (a) off-site vortex in the middle of the first BZ, and (b) on-site vortex at the edge of the first BZ, shown together with their phase structures.

the low density core on a constant density background. In a condensate loaded into an "infinite" optical lattice, a single-charge vortex can be stabilized in the form of a "dark" *Bloch vortex* on a periodic background of a Bloch state. Two examples of stationary Bloch vortices found by numerical solution [2, 15] of the time-independent version of Eq. (1) are shown in Fig. 1(a,b). Bloch vortices on the background of the ground lattice state [i.e. at the lowest edge of the first band, Fig. 1(a)] have the winding structure of the phase typical for a charge one vortex in a homogeneous condensate, due to the *trivial phase* of the background Bloch state [1, 5]. In contrast, the Bloch vortex residing on the excited Bloch state at the edge of the 1-st BZ with *nontrivial phase* develops a highly unusual phase pattern [Fig. 1(b)]. The phase winding around the zero density centre is  $2\pi$ .

The "dark" vortices on the ground (Bloch) state were found to be dynamically stable in [16, 17], although their experimental observation could be difficult because their core size is of the order of the lattice period. Recent analysis of the Bose-Hubbard model for a strongly correlated bosonic system with nearest neighbor repulsion in an optical lattice [18] also revealed the existence of a

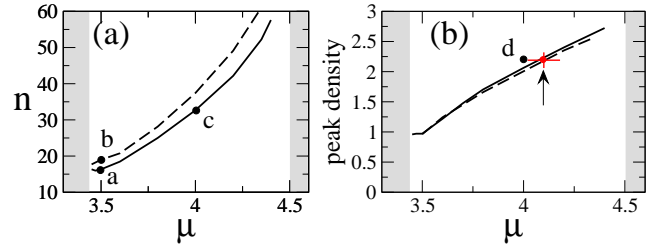


FIG. 2: Variations of (a) normalized atom number and (b) peak density of the on-site (solid) and off-site (dashed) gap vortex within the complete gap (open area) at  $V_0 = 3$ . Shaded areas are spectral bands. Examples of the spatial structure of the vortices at the marked points are shown in Fig. 3.

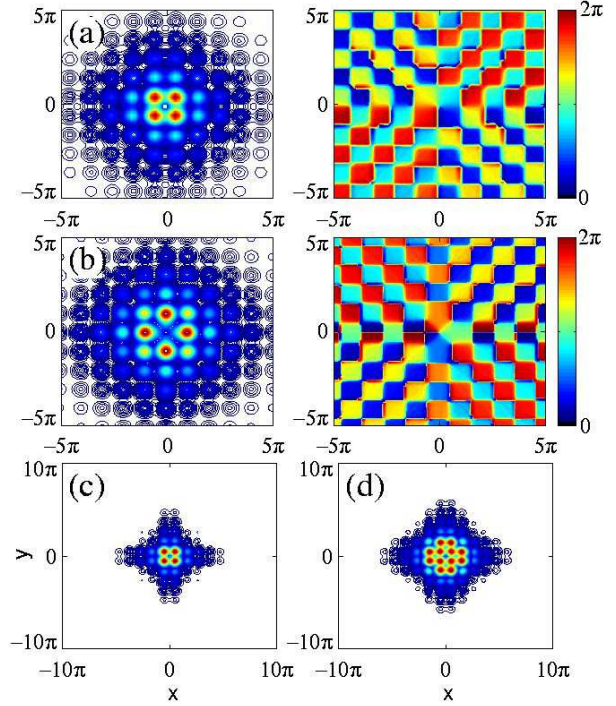


FIG. 3: (a,b) Density,  $|\psi|^2$ , and phase structure of the off-site (a) and on-site (b) gap vortices at marked points on the existence curves in Fig. 2. (c) Typical profile of a strongly localized off-site vortex (at  $\mu = 4.0$ ). (d) Example of a strongly localized broad off-site vortex (at  $\mu = 4.0$ ,  $n = 124$ ), with the parameters off the scale of Fig. 2(a), but peak density shown in Fig. 2(b), point "d". Red color codes maximum density.

single vortex with the particle density that can be either suppressed or *enhanced* in the vortex core.

Quite apart from the spatially delocalized states within the Bloch bands described above, *spatially localized* states of BEC with repulsive interactions can only exist within the complete spectral gaps [2, 5]. By imposing the vortex-like phase structure onto a spatially localized envelope of a Bloch state at the *M*-edge of the spectral gap (i.e. in the vicinity of the point *b* in Fig. 1), we have found, numerically, different families of spatially lo-

calized "bright" matter-wave gap vortex solitons characterized by the dependence of the (normalized) number of atoms in the localized state,  $n = \int |\psi|^2 dx dy$ , on the chemical potential [see Fig. 2(a)]. Akin to the bright gap matter-wave solitons [19], gap vortices have a clear atom number cut-off below which they undergo a delocalizing transition. The lowest energy families shown in Fig. 2 correspond to the on-site (localized on the lattice minimum) and off-site (localized on the lattice maximum) stationary gap vortices shown in Figs. 3(a,b) respectively. The peak density of the localized state is a function of chemical potential within the gap, as shown in Fig. 2(b), however the width (FWHM) of the high-density vortex core practically does not change across the gap. Gap vortices are strongly localized in the middle of the gap [see Fig. 3(c)], but near the top ( $X$ ) edge of the complete gap they develop extended tails that have the amplitude and phase structure of the background Bloch state.

Strongly localized core of the gap vortex is similar to vortex "cells" that were predicted to exist in tightly binding photonic lattices optically-induced in a *focusing* nonlinear medium [10]. Here, we find that the "elementary" vortex cells of two basic types form broader gap vortices by "tiling" the square lattice in a symmetric manner [c.f. Figs. 3 (c) and (d)]. The width of the gap vortex core is an additional parameter which characterizes higher-order families of the vortex states, however the peak density,  $n_{\max} \equiv |\psi|_{\max}^2$ , of the vortex core varies very little between "elementary" and broad vortices [see point *d* in Fig. 2(b) indicating the peak density of the vortex in Fig. 3(d)]. The high-density core of a broad gap vortex preserves characteristic phase structure of a vortex "cell", with its  $2\pi$  winding structure, whereas its tails are characterized by a *nontrivial phase pattern* associated with the nontrivial phase of the underlying Bloch state, as seen in Figs. 3(a,b).

The localized states near the  $M$  edge of the complete gap can be described by the trial function:

$$\psi(x, y) = Ar^m \exp(-r^2/a^2 + i\phi) B_1(x, y), \quad (2)$$

where  $r^2 = x^2 + y^2$ , and  $B_1(x, y)$  is the Bloch state at the lower edge of the first gap. The Bloch state at the respective edge is always out-of-phase with the lattice potential, and due to separability of the lattice potential it can be well approximated as  $B_1 \approx \cos(x+\theta) \cos(y+\theta)$  (see, e.g. [1]), where  $\theta$  is a shift of the vortex center relative to the lattice minimum. The approximate form of the on-site and off-site vortex configurations is well captured by the trial function (2) with  $m = 2$ ,  $\theta = 0$ , and  $m = 1$ ,  $\theta = \pi/2$ , respectively. In both cases the necessary condition for the existence for a stationary state, i.e. zero linear momentum [20]  $\int \text{Im}(\psi^* \nabla \psi) dx dy = 0$ , is satisfied in the limit of  $a \gg 1$ . The characteristic width of the gap vortex is given by  $a = p\pi$ , where integer  $p$  determines the size of the high-density vortex core in lattice periods. The examples of exact numerical solutions of well-localized

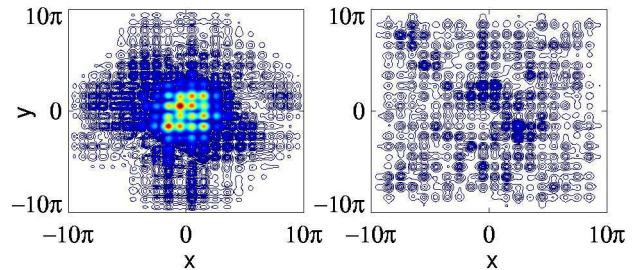


FIG. 4: Snapshots of the density distribution for a dynamically unstable wide off-site vortex in Fig. 3(d) at evolution times  $t=252$  (left) and  $t=600$  (right).

off-site vortices corresponding to  $p = 1$  and  $p = 2$  are presented in Figs. 3(c,d), respectively.

By direct numerical simulations of Eq. (1) we have confirmed that both the off-site and on-site gap vortices can be dynamically stable. The phase distribution evolves and the phase dislocation *precesses* around the centre of the vortex, whereas the vortex magnitude and polarity of its charge are *preserved* in time. In contrast, broad gap vortices characterized by much higher atom numbers in the localized state are *dynamically unstable*, and experience rapid delocalization at relatively long evolution times, as shown in Fig. 4. This process also destroys the phase structure of the gap vortex core.

Finally, we discuss the feasibility of dynamical generation of gap vortices in an experiment. To date, generation of nonlinear localized states of BEC in the form of a *bright gap soliton* has been successfully achieved in a 1D optical lattice [8], near the edge of the first BZ. The key to the success of that experiment was a low atom number ( $N \sim 10^2$ ) that allowed generation of a fundamental gap soliton near the band edge. In contrast to the 1D case, the existence of the particle number threshold for the localized states in 2D [19] means that the generation process can fail for insufficient initial atom numbers [21]. Our analysis shows that the key ingredients to successful generation of the gap vortex are: (i) preparation of the BEC wavepacket at the edge  $M$  of the first BZ, (ii) initial number of atoms well exceeding the threshold atom number for gap vortices, and (iii) the peak density of the BEC wavepacket being above the threshold peak density for a gap vortex. While the requirements (i) and (ii) are quite intuitive, the requirement (iii) is most stringent. To demonstrate the dramatic role of the peak density thresholds, we impose a  $2\pi$  phase winding ramp onto a broad wavepacket near the edge of the first BZ and explore its evolution in the dynamical simulations of the Eq. (1). We therefore assume that, initially, the wave function has a form given by Eq. (2) with  $m, \theta = 0$ , and a typical density distribution shown in Fig. 5(a). The numerical simulations of the mean-field model in [21] suggest that the preparation (and localization) of the ini-

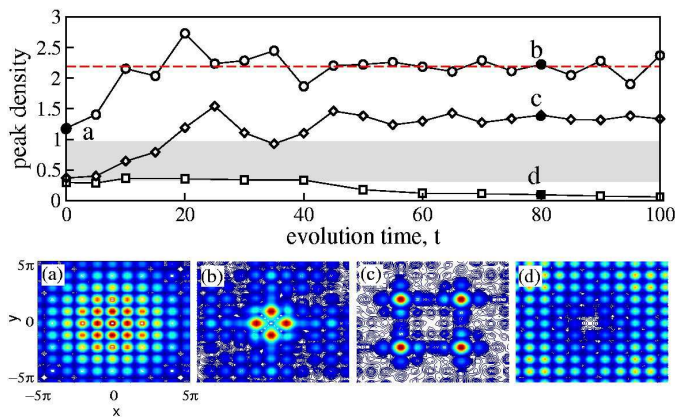


FIG. 5: Top: Evolution of the peak density of a BEC wavepacket with the initial peak density (circles) above threshold for generation of the gap vortices, (diamonds) below the gap vortex threshold but above the bright gap soliton threshold, and (squares) below bright gap soliton threshold ( $V_0 = 3.0$ ). Bottom: Snapshots of the condensate density at marked points: (a) an initial wavepacket, (b) generated on-site gap vortex with the phase structure (not shown) of Fig. 3(b), (c) generated weakly bound steady state of four bright gap solitons, and (d) discrete diffraction.

tial BEC wavepacket in the above form can be achieved via an adiabatic process of driving condensate to the  $M$  edge of the BZ with subsequent expansion in the lattice. The phase dislocation can be subsequently imprinted by a laser field [22]. The results of the numerical simulations for a shallow lattice ( $V_0 = 3.0$ ), with  $a = 4.5\pi$  and  $A = 1.2, 0.7$ , and  $0.6$  are presented in top panel of Fig. 5 by curves (b), (c), and (d), respectively. In the cases (b), (c), and (d) the initial number of atoms exceeds the threshold atom number value for generation of an on-site gap vortex by 9, 2, and 1.7 times, respectively. However, the initial peak density in the case (b) lies *above* the gap vortex threshold, in the case (c) it is in the *intermediate* domain (shaded area in Fig. 5, top) between the thresholds for a gap vortex and a bright gap soliton, and in the case (d) the peak density is only *marginally below* the threshold for generation of a bright gap soliton.

The results of the initial state evolution are shown in Fig. 5, bottom. In the case (b), the on-site gap vortex is generated in the transient process where the BEC density distribution is evolving around a vortex state with the peak density of  $n_{\max} \approx 2.2$ , marked by a dashed line in Fig. 5. The one-to-one correspondence between the peak density of a stationary gap vortex state and its chemical potential [see Fig. 2(b)] allows us to determine the approximate chemical potential (with standard deviation) of the generated on-site vortex state [pointed at by an arrow in Fig. 2(b)], and identify it as a *well-localized gap state*. Only approximately 40% of the initial atom numbers are retained in the localized state. Growth in the initial number of atoms, i.e. due to a greater width of the initial wavepacket, leads to the increasing deviations

from the average state, and to larger uncertainties in both  $\mu$  and  $n_{\max}$  of the generated vortex. In the case shown in Fig. 5(c) a weakly bound state of bright gap vortices forms, with an arbitrary phase relationship between the soliton peaks. The retention of atoms in the localized states is almost 90%. In the case (d) the localized states do not form and instead the discrete diffraction of the initial state is observed.

In conclusion, we have predicted novel types of localized vortex states of repulsive BECs in optical lattices, and identified the key requirements for their generation. Our results provide the next step in understanding the complex interplay between the superfluid behavior of a BEC with its inherent signatures, such as vorticity, and the nonlinear behavior of coherent matter waves in periodic potentials. The experimental observation of predicted structures seems feasible in view of the recent observation of a 2D BEC in an optical surface trap, and the fascinating prospects of the creation of optical surface lattices [23]. Our predictions are also relevant to the light beams carrying phase dislocations in 2D photonic structures with a defocusing nonlinearity.

- 
- [1] H. Pu *et al.*, Phys. Rev. A **67**, 043605 (2003).
  - [2] E.A. Ostrovskaya and Yu.S. Kivshar, Phys. Rev. Lett. **90**, 160407 (2003).
  - [3] B. Eiermann *et al.*, Phys. Rev. Lett. **91**, 060402 (2003).
  - [4] L. Fallani *et al.*, Phys. Rev. Lett. **91**, 240405 (2003).
  - [5] E.A. Ostrovskaya and Yu.S. Kivshar, Opt. Express **12**, 19 (2004).
  - [6] O. Zobay *et al.*, Phys. Rev. A **59**, 643 (1999).
  - [7] P.J. Louis *et al.*, Phys. Rev. A **67**, 013602 (2003).
  - [8] B. Eiermann *et al.*, arXiv:cond-mat/0402178 (2004).
  - [9] J.E. Williams and M.J. Holland, Nature (London) **401**, 586 (1999); M.R. Matthews *et al.*, Phys. Rev. Lett. **83**, 2498 (1999).
  - [10] J. Yang and Z. H. Musslimani, Opt. Lett. **28**, 2094 (2003); J. Yang, arXiv:nlin.PS/0310024 (2003).
  - [11] B.B. Baizakov *et al.*, Europhys. Lett. **63**, 642 (2003).
  - [12] T.J. Alexander *et al.*, arXiv:physics/0403103 (2004).
  - [13] A. Ferrando *et al.*, Opt. Express **12**, 817 (2004).
  - [14] D. N. Neshev *et al.*, Phys. Rev. Lett. **92**, 123903 (2004).
  - [15] J.J. Garcia-Ripoll and V.M. Pèrez-García, SIAM J. Sci. Comput. **23**, 1316 (2001).
  - [16] A. B Bhattacharjee *et al.*, arXiv:cond-mat/0312124 (2003).
  - [17] P.G. Kevrekidis *et al.*, J. Phys. B, **36**, 3467 (2003).
  - [18] C. Wu *et al.*, Phys. Rev. A **69**, 043609 (2004).
  - [19] see B. B. Baizakov and M. Salerno, Phys. Rev. A, **69**, 013602 (2004); N. K. Efremidis *et al.*, Phys. Rev. Lett., **91**, 213906 (2003), and references therein.
  - [20] A. S. Desyatnikov and Yu. S. Kivshar, J. Opt. B, **4**, 58 (2002).
  - [21] A. M. Dudarev *et al.*, arXiv:cond-mat/0312054 (2003).
  - [22] L. Dobrek *et al.*, Phys. Rev. A **60**, R3381 (1999).
  - [23] D. Rychtarik *et al.*, Phys. Rev. Lett. **92**, 173003 (2004).